

Propene Adsorption Sites in Zeolite ITQ-12: A Combined Synchrotron X-ray and Neutron Diffraction Study

Xiaobo Yang,^{*,†,‡} Brian H. Toby,[‡] Miguel A. Camblor,[§] Yongjae Lee,^{||} and David H. Olson^{†,⊥}

Department of Chemical and Biomolecular Engineering, University of Pennsylvania, Philadelphia, Pennsylvania 19104, NIST Center for Neutron Research, National Institute of Standards and Technology (NIST), Gaithersburg, Maryland 20899, Instituto de Ciencia de Materiales de Madrid (CSIC), Departamento de Materiales Porosos y Compuestos de Intercalación, Campus Cantoblanco, 28049 Madrid, Spain, and Physics Department, Brookhaven National Laboratory, Upton, New York 11973-5000

Received: February 14, 2005

The adsorption site of propene in the small-pore, pure silica zeolite [Si₂₄O₄₈]-ITW-ITQ-12 has been characterized via Rietveld refinement of the crystal structure of propene-loaded ITQ-12 on the basis of synchrotron X-ray and neutron diffraction data taken at 298 K. The structure can be described with a monoclinic unit cell having *Cm* symmetry and unit cell parameters *a* = 10.436 Å, *b* = 15.018 Å, *c* = 8.855 Å, β = 105.74°, and volume = 1335.9 Å³. Four-fold disordered adsorption sites that are nearly equivalent relative to the cage's 2/*m* pseudosymmetry are located near the center of each ellipsoidally shaped [4⁴5⁴6⁴8⁴] cage. At this site, the adsorbed propene molecule lies on a plane close and approximately parallel to the equatorial plane of the cage and is aligned with its methylene group pointing toward the pore's eight-ring window. The refined propene concentration, 1.8 per unit cell content, is close to one propene molecule per [4⁴5⁴6⁴8⁴] cage and the amount observed in adsorption experiments at 298 K and 1 atm propene partial pressure.

Introduction

The separation of propene from mixtures with propane is an important process in the petrochemical industry, currently performed by fractional distillation.¹ Because of the very close volatility of these two hydrocarbons, the process is energy intensive and difficult to accomplish. In recent years, several alternative separation processes have been investigated on the basis of the pressure-swing adsorption (PSA) method.² Adsorbents proposed for this purpose include modified silica gel,³ zeolite A,⁴ aluminum phosphate,^{4–6} and gallium phosphate⁶ molecular sieves and a number of high or pure silica zeolites.^{7–11} Among them, small-pore (eight-membered ring) pure silica zeolites exhibit superb properties, promising advantages over other adsorbents for the separation of the light hydrocarbon gases. Pure silica zeolites are highly stable, hydrophobic, free of acidic sites, and free from coke formation. Furthermore, eight-ring pore apertures are close to the size of the C₃ hydrocarbon molecules and discriminate, because of steric effects, the slightly larger propane from propene, resulting in large differences in diffusion rates. The ratios of diffusion coefficients for propene and propane, e.g., in pure silica chabazite, can be as large as

46 000 at 303 K.^{8,9} These properties are essential for an effective kinetic-based propene/propane PSA separation.

[Si₂₄O₄₈]-ITW-ITQ-12 is a new pure silica zeolite recently reported by Boix et al.^{10,12} Its structure contains ellipsoidal [4⁴5⁴6⁴8⁴] cavities that are linked together by double four-membered rings and interconnected via eight rings. There are two sets of eight-membered ring windows accessing the cavities, one is too narrow (2.4 × 5.3 Å) to allow the passage of even the smallest hydrocarbon, while the other one is more circular (3.8 × 4.1 Å), forming a 1D channel system, which allows propene and propane to pass through but at different diffusion rates.^{10,11} For a detailed understanding of the propene adsorption behavior and possible structural interactions between the zeolite lattice and sorbate molecules, characterizations of the adsorption sites are required. Rietveld analysis based on X-ray and neutron diffraction data has been employed to characterize the structure of zeolites loaded with hydrocarbon guest species. Recent examples are the locations of adsorption sites of chlorofluorocarbons in zeolite NaY,¹³ NaX,¹⁴ *n*-hexane in silicalite-1,¹⁵ etc. Usually, the diffraction experiments are performed at low temperatures (liquid helium to liquid nitrogen temperatures), “freezing” the thermal motions of the guest molecules, to achieve a clear characterization of their position and orientation. However, this approach is not applicable to the present study because it is evidenced that the framework structure of zeolite ITQ-12 is quite flexible. Its unit cell dimension is sensitive to temperature.¹¹ The propene adsorption sites, which would be located by using low-temperature data, could be very different from, and thus not represent, the real situations at conditions in which the separation processes are carried out, i.e., 298–353 K. Fortunately, the [4⁴5⁴6⁴8⁴] cage of ITQ-12 is slit-shaped and very narrow. The thermal motions of an organic molecule inside

* Author to whom correspondence should be addressed. E-mail: Xiaobo.Yang@pci.uni-hannover.de. Telephone: +49-511-762 3080. Fax: +49-511-762 19121.

† University of Pennsylvania.

‡ NIST Center for Neutron Research.

§ Instituto de Ciencia de Materiales de Madrid (CSIC).

|| Brookhaven National Laboratory.

⊥ Present address: Rutgers University, Department of Chemistry and Chemical Biology, 610 Taylor Road, Piscataway, New Jersey 08854.

* Present address: Institute of Physical Chemistry and Electrochemistry, University of Hanover, D-30167 Hanover, Germany.

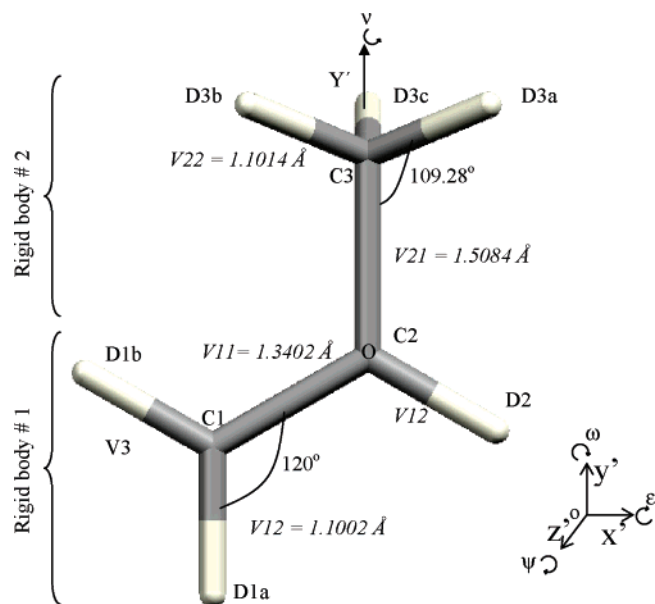


Figure 1. The original rigid body settings for description of an adsorbed propene molecule in ITQ-12

can be very confined. Through proper treatments during the Rietveld analysis, such as using carefully designed rigid body constraints, it is possible to model and simulate the position and orientation of the guest species, even at these relatively high temperatures. Recently, we reported the position of the structure-directing agents, 1,3,4-trimethylimidazolium cation and fluoride anion in the zeolite ITQ-12, as determined by the Rietveld refinement using synchrotron X-ray diffraction data at 298 K.¹⁶ In the current study, synchrotron X-ray and neutron diffraction experiments are performed on powder samples of zeolite ITQ-12 with preadsorbed propene and deuterated propene, respectively. The purpose is to locate the position of the adsorbed propene molecules at 298 K and to observe a corresponding change of the unit cell parameters upon propene adsorption.

Experimental Section

Zeolite ITQ-12 was synthesized following the procedure described in refs 10, 12, and 16 with tetraethyl orthosilicate in the presence of 1,3,4-trimethylimidazolium cations and fluoride anions.

Synchrotron X-ray Diffraction. After calcination at 1023 K, ITQ-12 powder was packed into a glass capillary of 0.3 mm diameter, evacuated at 573 K for 1 h, exposed to 1 atm (101.3 kPa) propene for 1 h at 298 K, and then sealed.

The synchrotron X-ray powder diffraction data were collected at 298 K at the beamline X7A of the National Synchrotron Light Source at Brookhaven National Laboratory. Monochromatic synchrotron X-ray radiation ($\lambda = 0.6642(1)$ Å) was used in conjunction with a gas-proportional position-sensitive detector. The sample capillary was spun for better powder averaging, and the PSD was stepped in 0.25° intervals between 1 and 50° to produce 0.01° step scan data.

Neutron Diffraction. Calcined zeolite ITQ-12 was evacuated at 573 K for 1 h and transferred, in a glovebox containing dry helium, into a vanadium can for the neutron diffraction experiment. A total amount of 2.8 g powder sample was loaded into the can. Then the can was connected to a vacuum line, evacuated at 298 K, exposed to 1 atm deuterated propene (C_3D_6) for ~ 15 min at 298 K, and then sealed.

Neutron diffraction data in the constant-wavelength mode were recorded at 298 K at the Center for Neutron Research, the National Institute of Standards and Technology. The wavelength used was $2.0787(2)$ Å. The pattern was scanned over the 2θ range $3-161.85^\circ$ at 0.05° steps.

Rietveld Refinement. Combined Rietveld refinement based on the synchrotron X-ray and neutron diffraction data was performed with the GSAS program¹⁷ and the EXPGUI graphical interface.¹⁸ A total of 4599 X-ray diffraction data points in the 2θ range $4-50^\circ$, and 2979 neutron diffraction data points from 11 to 160° were included for the refinement. For both patterns, the background was fitted using shifted Chebyshev functions with 19 coefficients. The X-ray peak profile was simulated using a modified pseudo-Voigt function with the Finger-Cox-

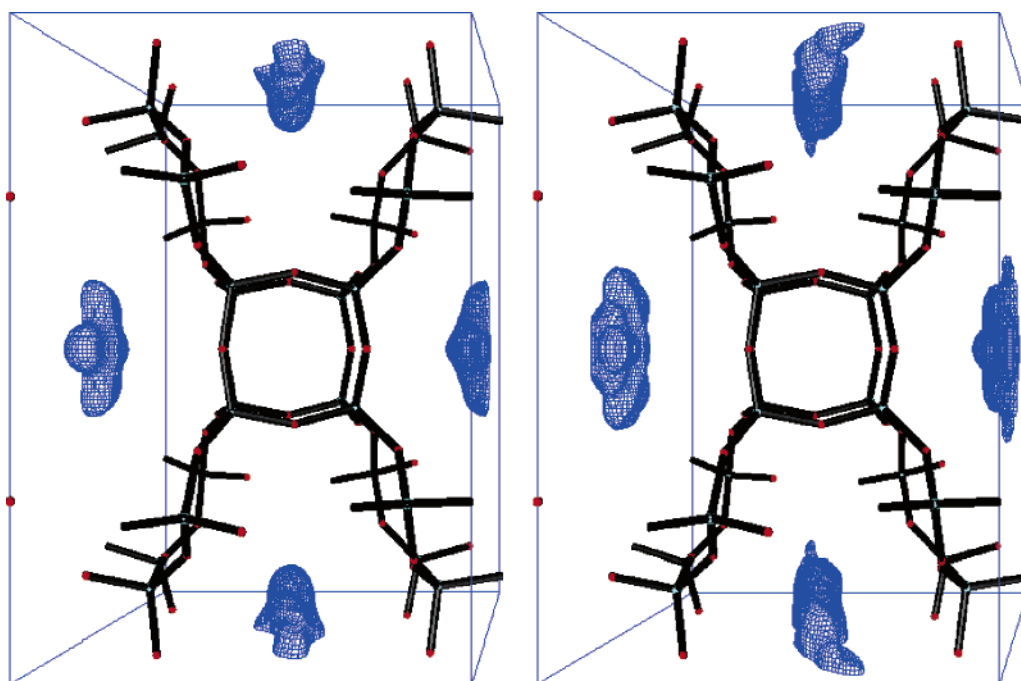


Figure 2. Difference Fourier maps calculated from the Rietveld refinement with ITW framework model, unit cell viewing down the Z-axis. Left: the map based on synchrotron X-ray diffraction data; right: neutron diffraction data.

TABLE 1: Crystallographic and Experimental Parameters for Rietveld Refinement for Zeolite ITQ-12 with Adsorbed Propene

	synchrotron X-ray diffraction	neutron diffraction
wavelength (Å)	0.6642	2.0804(1)
temperature (K)	298	298
2θ range (deg)	1–55 (used 4–50)	3–162 (used 11–160)
step size (deg)	0.01	0.05
no. of data points	4599	2979
no. of reflections	1617	639
space group	<i>C1m1</i> (no. 8)	
unit cell parameters (Å)		
<i>a</i>	10.43638(19)	
<i>b</i>	15.01832(27)	
<i>c</i>	8.85531(18)	
β (deg)	105.7386(11)	
cell volume (Å ³)	1335.92(4)	
residuals		
<i>R</i> _{wp}	0.0324	0.0730
<i>R</i> _p	0.0261	0.0580
<i>R</i> _F ²	0.0566	0.0988
reduced χ ²	18.92	

Jephcoat correction¹⁹ to account for asymmetry of low-angle peaks due to axial divergence (Function Type 3 in GSAS). The neutron profile was fitted using a modified Gaussian function with one axial divergence asymmetry parameter. The unit cell model of the ITQ-12 framework, in *Cm* symmetry as per Ref 16, was used as the starting model. During the refinement, soft constraints were applied to the Si–O bond lengths, 1.610 Å, with tolerance values (*σ*) and overall weight (FACTR) of 0.002 and 1, respectively. Upon reaching a good fit of the simulated to the experimental diffraction patterns, difference Fourier maps were calculated to locate the propene adsorption sites. The propene molecule was then introduced into the model as two coupled rigid bodies sharing an origin at the position C2 (Figure 1). The first rigid body has two translational lengths, determining the C1=C2 double bond length (V11) and the length of the C–D bonds (V12) connected to those two C atoms, respectively. The second rigid body model consists of the C3 atom and its bonding hydrogen atoms with translational lengths V21 for C2–C3 and V22 for C3–D3. An additional variable parameter allows the rotation of C2–C3 *σ*-bond in rigid body number 2. This coupled pair of rigid bodies has a total of 11 potential refinable parameters. The origin location and the orientation of the body contribute six degrees of freedom. Two sets rigid bodies of this kind were inserted into the cage of ITQ-12 framework. All positional parameters, site occupancy factors, and bond lengths were refined. To reduce the overall number of variables, isotropic thermal displacement factors were constrained to be the same for each type of atom. Site occupancy factors for the atoms of each propene molecule were constrained to be the same. Final Rietveld cycles included a total of 121 refined parameters, of which 65 are structural.

Cerius² Simulation. A molecular simulation of the equilibrium of propene adsorption in ITQ-12 at 298 K and 106.7 kPa (close 1 atm) was carried out using the Cerius² Adsorption Module of Accelrys with the pccf_300_1.01 force field²⁰ and using the framework structure model of ITQ-12 in *Cm* symmetry, obtained from a Rietveld fit.¹⁶ Positions of adsorbed propene molecules were generated with the Monte Carlo method on a model consisting of 4 × 3 × 5 unit cells and were accepted if energetically favored. Five million configurations were sufficient to bring the system to equilibrium.

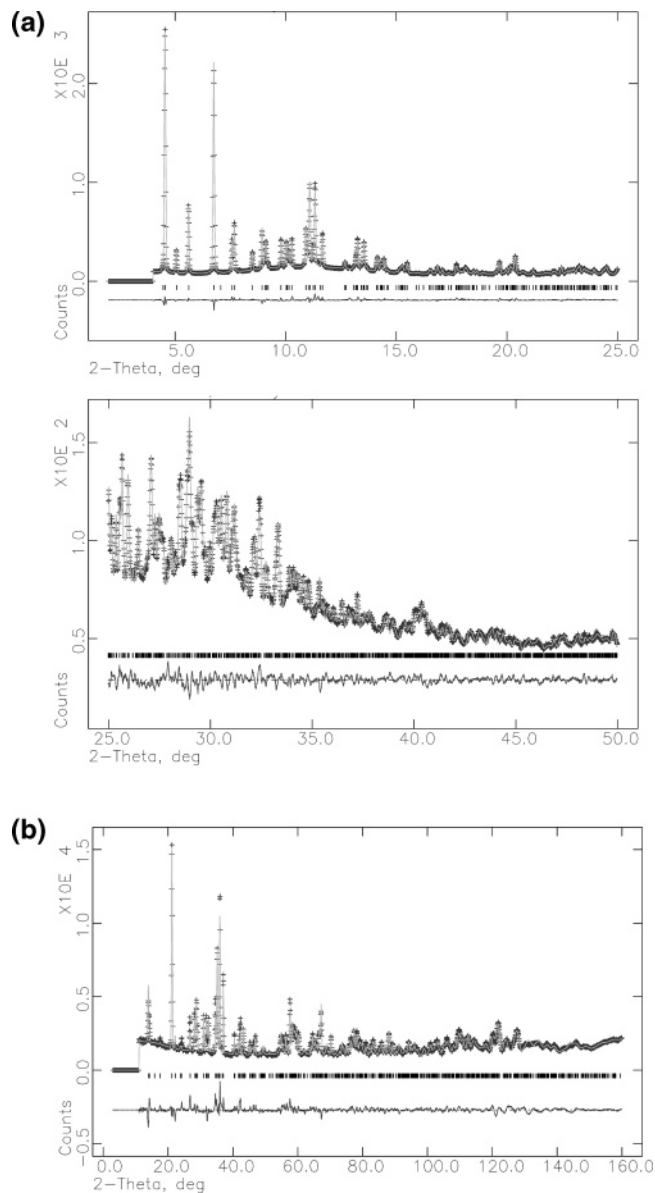


Figure 3. (a) Observed (+) and calculated (solid line) synchrotron X-ray diffraction patterns of ITQ-12 with adsorbed propene. Vertical marks indicate the positions of allowed reflections. The lower trace is the difference plot. Refined $\lambda = 0.6642$ Å. (b) Observed (+) and calculated (solid line) neutron diffraction patterns of ITQ-12 with adsorbed propene. Vertical marks indicate the positions of allowed reflections. The lower trace is the difference plot. Refined $\lambda = 2.0804(1)$ Å.

Results and Discussion

Rietveld Refinement. The ITW-type framework structure of zeolite ITQ-12 has been solved and described with a monoclinic unit cell in the *Cm* symmetry.^{10,16} Unit cell parameters, refined from synchrotron X-ray data for calcined ITQ-12, have been reported as $a = 10.336$ Å, $b = 15.018$ Å, $c = 8.864$ Å, $\beta = 105.36^\circ$, and cell volume = 1326.8 Å³ at 298 K.¹⁶ The unit cell composition is [Si₂₄O₄₈]. Iterating the Rietveld cycles for propene-loaded ITQ-12 using this silica framework model without an inclusion of the adsorbed guest molecule yields a fit to the diffraction patterns with residual values: $R_{wp} = 0.1189$, $R_p = 0.0729$ for X-ray and $R_{wp} = 0.1829$, $R_p = 0.1138$ for neutron. Difference Fourier maps calculated at this stage are illustrated in Figure 2. In both maps, on the basis of X-ray and neutron diffraction data, respectively, groups of electron or nuclear density peaks appear around the center of

TABLE 2: Atomic Positions, Isotropic Thermal Displacement Factors, and Site Occupancy Factors for ITQ-12 with Adsorbed Propene in the Unit Cell of Space Group *Cm*

name	X	Y	Z	$U_{\text{iso}} \times 100$	SOF	name	X	Y	Z	$U_{\text{iso}} \times 100$	SOF
Si1	0.643812	0.250943	0.112157	0.53(3)	1	Si4	-0.65404(34)	0.23827(26)	-0.0962(4)	0.53(3)	1
Si2	0.68834(91)	0.40196(30)	0.6741(9)	0.53(3)	1	Si5	-0.70315(90)	0.39517(28)	-0.6669(9)	0.53(3)	1
Si3	0.58727(94)	0.40045(29)	0.3206(9)	0.53(3)	1	Si6	-0.60653(91)	0.39416(26)	-0.3010(9)	0.53(3)	1
O7	0.6586(11)	0.3399(5)	0.2168(12)	0.97(5)	1	O14	0.6020(18)	0.5	0.2531(15)	0.97(5)	1
O8	0.4311(10)	0.3736(9)	0.2812(17)	0.97(5)	1	O15	-0.8182(13)	0.3375(5)	-0.7836(12)	0.97(5)	1
O9	0.6665(13)	0.3687(6)	0.4958(9)	0.97(5)	1	O16	-0.6228(18)	0.5	-0.2794(16)	0.97(5)	1
O10	0.7444(15)	0.2632(6)	0.0076(19)	0.97(5)	1	O17	-0.6503(11)	0.3352(5)	-0.1731(13)	0.97(5)	1
O11	0.7302(17)	0.5	0.7458(15)	0.97(5)	1	O18	-0.4497(10)	0.3753(8)	-0.2843(17)	0.97(5)	1
O12	0.5000(6)	0.2268(4)	-0.0013(16)	0.97(5)	1	O19	-0.6893(13)	0.3867(6)	-0.4828(9)	0.97(5)	1
O13	0.8039(13)	0.3347(6)	0.7666(12)	0.97(5)	1	O20	-0.7353(19)	0.5	-0.6886(15)	0.97(5)	1
C1	0.4386(19)	-0.0056(18)	0.3040(21)	5.0(6)	0.225(2)	D1a	0.4004(36)	0.0495(24)	0.2224(23)	7.5(9)	0.225(2)
D1b	0.4402(25)	-0.0738(21)	0.2589(29)	7.5(9)	0.225(2)						
C2	0.4833(23)	0.0103(11)	0.4584(21)	5.0(6)	0.225(2)	D2	0.5215(42)	-0.0449(12)	0.5400(26)	7.5(9)	0.225(2)
C3	0.4812(33)	0.1037(11)	0.5202(30)	5.0(6)	0.225(2)	D3b	0.5583(51)	0.1109(17)	0.6324(40)	7.5(9)	0.225(2)
D3a	0.5007(56)	0.1518(12)	0.4352(45)	7.5(9)	0.225(2)	D3c	0.3831(42)	0.1178(19)	0.5388(62)	7.5(9)	0.225(2)
C1B	0.5030(26)	-0.0056(18)	0.6377(22)	5.0(6)	0.225(2)	D1bB	0.5015(33)	-0.0738(21)	0.6827(31)	7.5(9)	0.225(2)
D1aB	0.5413(42)	0.0495(24)	0.7193(22)	7.5(9)	0.225(2)						
C2B	0.4584(21)	0.0103(11)	0.4833(23)	5.0(6)	0.225(2)	D2B	0.4202(39)	-0.0449(12)	0.4017(29)	7.5(9)	0.225(2)
C3B	0.4605(28)	0.1037(11)	0.4215(30)	5.0(6)	0.225(2)	D3bB	0.3834(45)	0.1109(17)	0.3093(41)	7.5(9)	0.225(2)
D3aB	0.4410(54)	0.1518(12)	0.5064(45)	7.5(9)	0.225(2)	D3cB	0.5586(36)	0.1178(19)	0.4029(59)	7.5(9)	0.225(2)

TABLE 3: Bond Lengths and Angles of ITQ-12 with Adsorbed Propene as Refined in the *Cm* Unit Cell^a

atom Pair	distance (Å)	angle (deg)	atom Pair	distance (Å)	angle (deg)		
Si1-O7	1.609(4)	O7-Si1-O10	105.3(6)	Si1-O15	1.605(4)	O10-Si1-O12	108.4(9)
Si1-O10	1.5878(35)	O7-Si1-O12	118.4(6)			O10-Si1-O15	109.4(7)
Si1-O12	1.605(4)	O7-Si1-O15	112.7(7)			O12-Si1-O15	102.5(6)
Si2-O9	1.612(4)	O9-Si2-O11	128.2(7)	Si2-O18	1.631(4)	O11-Si2-O13	106.6(6)
Si2-O11	1.616(4)	O9-Si2-O13	101.0(5)			O11-Si2-O18	107.2(9)
Si2-O13	1.615(4)	O9-Si2-O18	104.3(7)			O13-Si2-O18	108.4(6)
Si3-O7	1.612(4)	O7-Si3-O8	109.2(5)	Si3-O14	1.633(4)	O8-Si3-O9	110.8(7)
Si3-O8	1.622(4)	O7-Si3-O9	100.7(5)			O8-Si3-O14	109.7(9)
Si3-O9	1.620(4)	O7-Si3-O14	101.8(5)			O9-Si3-O14	123.1(7)
Si4-O10	1.5804(34)	O10-Si4-O12	115.3(9)	Si4-O17	1.612(4)	O12-Si4-O13	110.6(6)
Si4-O12	1.608(4)	O10-Si4-O13	109.9(8)			O12-Si4-O17	100.5(6)
Si4-O13	1.606(4)	O10-Si4-O17	110.8(6)			O13-Si4-O17	109.3(7)
Si5-O8	1.621(4)	O8-Si5-O15	105.2(6)	Si5-O20	1.6103(34)	O15-Si5-O19	117.2(6)
Si5-O15	1.608(4)	O8-Si5-O19	115.2(7)			O15-Si5-O20	110.8(5)
Si5-O19	1.602(4)	O8-Si5-O20	109.2(9)			O19-Si5-O20	99.0(6)
Si6-O16	1.6154(34)	O16-Si6-O17	113.7(5)			Si2-O11-Si2	131.4(8)
Si6-O17	1.599(4)	O16-Si6-O18	107.2(8)			Si1-O12-Si4	159.3(5)
Si6-O18	1.628(4)	O16-Si6-O19	98.1(6)			Si2-O13-Si4	145.5(8)
Si6-O19	1.612(4)	O17-Si6-O18	108.3(5)			Si3-O14-Si3	132.6(8)
		O17-Si6-O19	119.4(6)			Si1-O15-Si5	147.2(8)
		O18-Si6-O19	109.4(7)			Si6-O16-Si6	159.5(11)
		Si1-O7-Si3	144.1(7)			Si4-O17-Si6	147.5(8)
		Si3-O8-Si5	141.7(8)			Si2-O18-Si6	149.9(8)
		Si2-O9-Si3	138.3(7)			Si5-O19-Si6	152.5(8)
		Si1-O10-Si4	172.5(7)			Si5-O20-Si5	155.7(12)
C1-C2 ^b	1.34044(3)	C1-C2-C3	120	C2-D2 ^d	1.10030(5)	C2-C3-D3	109.3
C2-C3 ^c	1.50927(3)	D1-C1-C2	120	C3-D3 ^e	1.10077(4)		
C1-D1 ^d	1.10030(5)	C1-C2-D2	120				

^a Soft constraints applied for Si-O distances at 1.610 Å, with $\sigma = 0.002$, overall weight factor = 1. ^b Refined rigid body translational length V11. ^c Refined rigid body translational length V21. ^d Refined rigid body translational length V12. ^e Refined rigid body translational length V22.

the ellipsoidal [4⁵4⁶8⁴] cage. These peaks are due to the propene molecules, which had not yet been modeled. Considering the approximately triangular shape of the propene molecule, the maps suggest the presence of more than the two molecular orientations that would be generated by placing a single species in the cage. The neutron map exhibits more features than the X-ray map because deuterium has a large scattering cross section for neutrons, while hydrogen or deuterium scattering is insignificant for X-rays.²¹ Attempts were made to model the structure with only one symmetry-related pair of propene molecules in the [4⁵4⁶8⁴] silica cage, but significantly, better fits were obtained with the addition of a second pair of propene. Noting that the [4⁵4⁶8⁴] silica cage has approximate 2/*m* symmetry and the approximate disk-shaped Fourier map features, it makes sense to relate the two pairs of guest molecules via a 2-fold axis at the center of the [4⁵4⁶8⁴] cage. Thus, the position of

the ellipsoidal [4⁵4⁶8⁴] cage. These peaks are due to the propene molecules, which had not yet been modeled. Considering the approximately triangular shape of the propene molecule, the maps suggest the presence of more than the two molecular orientations that would be generated by placing a single species in the cage. The neutron map exhibits more features than the X-ray map because deuterium has a large scattering cross section for neutrons, while hydrogen or deuterium scattering is insignificant for X-rays.²¹ Attempts were made to model the structure with only one symmetry-related pair of propene molecules in the [4⁵4⁶8⁴] silica cage, but significantly, better fits were obtained with the addition of a second pair of propene. Noting that the [4⁵4⁶8⁴] silica cage has approximate 2/*m* symmetry and the approximate disk-shaped Fourier map features, it makes sense to relate the two pairs of guest molecules via a 2-fold axis at the center of the [4⁵4⁶8⁴] cage. Thus, the position of

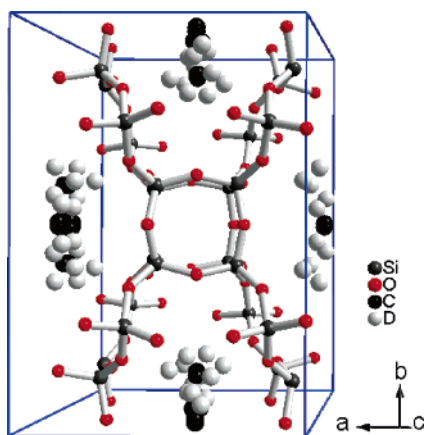


Figure 4. The Rietveld refined unit cell of ITQ-12 with adsorbed propene.

the second pair of molecules is fixed at (z, y, x) , relative to the first propene located at (x, y, z) . Furthermore, one more rotational axis, 180° around the Cartesian y axis of the rigid body origin, is forced to the second propene model to make it an operational result of the first one by the $2/m$ symmetry. The resulting model by this treatment contains four molecules of propene in each cage, which are related by $2/m$ symmetry. The model represents 4-fold disorder of the propene sites since one cage can only accommodate one propene molecule.

Incorporating this model for the guest species into further Rietveld refinement cycles, the residual values in the Rietveld fit have been drastically decreased to $R_{wp} = 0.0324$, $R_p = 0.0261$ for X-ray and $R_{wp} = 0.0730$, $R_p = 0.0580$ for neutron data. Experimental conditions and refinement results are summarized in Table 1. The calculated X-ray and neutron diffraction patterns, the experimental diffraction data, and their difference plots are presented in Figure 3. Atomic positions, site occupancy factors, and isotropic thermal displacement factors are shown in Table 2. Bond distances and angles in the unit cell calculated from the Rietveld refined structure model are given in Table 3. The refined unit cell parameters are: $a = 10.4364(2)$ Å, $b = 15.0183(3)$ Å, $c = 8.8553(2)$ Å, $\beta = 105.739(1)^\circ$, and unit cell volume = $1335.92(4)$ Å³. In the final refinements, X-ray and neutron data were weighted according to their statistical uncertainties and had a net contribution to the total χ^2 of 78% and 20%, respectively. Weighting for the framework interatomic distances were adjusted to provide the expected range in Si–O bond distances. These soft constraints contributed 2% toward the total χ^2 . Removal of these weak constraints resulted in unreasonable bond lengths, but did not change the R -factors significantly.

Description of the Adsorption Site for Propene. The unit cell with the modeled atoms of adsorbed propene is illustrated in Figure 4. Comparison of this structural drawing with the Fourier maps in Figure 2 reveals a good agreement. The occupancy of these C and D atomic sites is 0.225(2), consistent with a refined unit cell content of $[(C_3D_6)_{1.80(1)}][Si_{24}O_{48}]$, indicating a loading slightly below one molecule per $[4^45^46^48^4]$ cage. This loading is effectively identical with the Cerius² simulation for 298 K and 106.7 kPa, which yielded 117.16 propene molecules in $4 \times 3 \times 5$ unit cells, i.e., 0.98 molecules per cage. Both results are consistent with the experimental adsorption isotherm values previously published.^{10,11}

The propene thus is modeled in the Rietveld refinement with a 4-fold disorder and a center of mass close to the center of the $[4^45^46^48^4]$ cage. Figure 5 shows a propene molecule at one representative site among those four. The origin of the rigid body model (the position of atom C2) is at (0.4833(23), 0.0103(11), 0.4584(21)), while the cage center is (0.5, 0, 0.5). The rotational variables for the Cartesian axes at the rigid body origin have been refined as $\epsilon(X') = -237.55^\circ$, $\omega(Y') = 100.70^\circ$, $\varphi(Z') = -217.46^\circ$. An additional angle around Y as shown in Figure 1, representing the rotation of the C2–C3 σ -bond, has been refined as $\nu(Y') = 184.42^\circ$ from its original setting shown in Figure 1. At this site, the carbon chain of the propene molecule aligns on a plane almost parallel and very close to the equatorial plane of the ellipsoidally shaped $[4^45^46^48^4]$ cage, with the methylene group pointing to the eight-ring window in the direction of the channel. The other three propene sites are related by the imposed $2/m$ symmetry and again close to the equatorial plane of the cage, with the methylene group pointing to the eight-ring window of the channel. It is interesting to observe that the propene sites do not display a shape of a completely disordered and freely rotating disk. Rather, the disordering can well be described by the symmetrically related 4-sites, whereby the positions, orientational angles, and bond lengths of a propene molecule have been satisfactorily and reliably refined.

Cerius² molecular simulation confirms these propene site locations. In the model containing 60 unit cells, i.e., 120 ellipsoidal cages, all 117.16 propene molecules are adsorbed near cage centers and align almost parallel to cage walls at equilibrium. The orientation of individual propene molecule consists of any one of the four sites of the Rietveld model.

The $[4^45^46^48^4]$ cage exhibits a shape of a narrow slit. Adsorption of propene results in an expansion of this slit in the x direction. The unit cell parameter a has increased from 10.336 Å to 10.436 Å upon propene adsorption, while b and c do not change significantly. At the refined adsorption site, some of the hydrogen atoms of propene approach framework oxygen

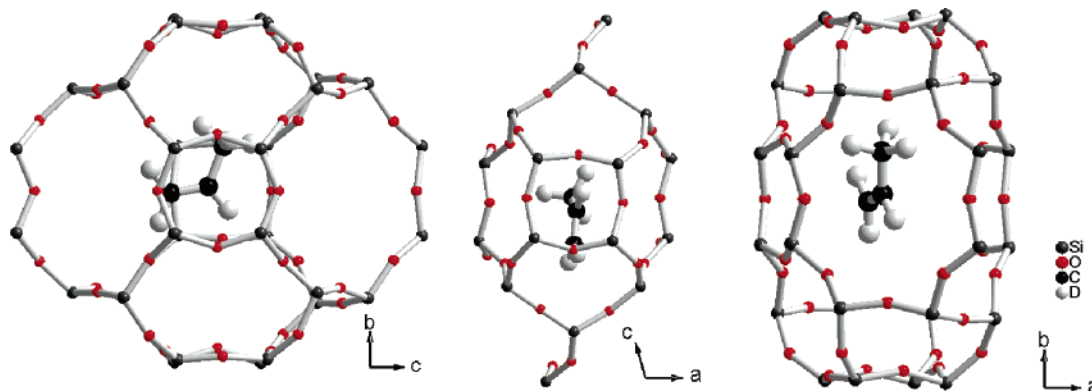


Figure 5. One representative propene adsorption site in the $[4^45^46^48^4]$ cage of ITQ-12, viewing down the x , y , and z axes, respectively.

TABLE 4: Short Contacts between Propene Hydrogen Atoms and Framework Oxygen Atoms

atom pair	distance (Å)	position of the O atom
D3c-O9	2.196	4-ring/6-ring
D3c-O13	2.481	6-ring/8-ring
D3cB-O19	2.547	4-ring/6-ring
D3cB-O7	2.379	6-ring/8-ring
D3cB-O15	2.444	6-ring/8-ring

atoms close to the sum of van der Waals radii, i.e., 2.40 Å (Table 4). This indicates the existence of strong interactions, e.g., H-bonds, between those atoms. These strong interactions may explain on one hand the restriction of the rotating freedom of adsorbed propene molecules. That is the reason the propene sites do not display a shape of a completely disordered disk. On the other hand, they would be reflected in high adsorption energy. Cerius² simulation results confirm that this is indeed the case: The isosteric adsorption heat for propene adsorption in ITQ-12 has been calculated as 40.9 kJ/mol, in agreement with the earlier reported experimental value.¹¹ This is higher than the value for other pure silica zeolites with slightly larger cages, e.g., the isosteric heat for propene adsorption in pure silica chabazite is 27.2 kJ/mol,⁹ and 36.0 kJ/mol for DD3R.⁷

Conclusions

Synchrotron X-ray and neutron diffractions have been performed on the small-pore pure silica zeolite ITQ-12 with preadsorbed propene at 298 K and 1 atm. On the basis of these data, Rietveld refinement of the crystal structure using carefully designed rigid body constraints has found a 4-fold disordered adsorption site close to the center of the [4⁴5⁴6⁴8⁴] cage, consistent with the 2/m pseudosymmetry of the cage. At the adsorption site, the propene molecule aligns with its C-C-C chain in a plane close and almost parallel to the equatorial plane of the ellipsoidally shaped cage, with the methylene group pointing toward the eight-ring window along the pore channel in the z direction. The refined unit cell content is |(C₃H₆)_{1.8}|[Si₂₄O₄₈], i.e., the adsorption capacity of ITQ-12 for propene under the applied conditions is very close to one molecule per [4⁴5⁴6⁴8⁴] cage. The adsorbed propene picks randomly any one

of the four nearly equivalent sites. The higher isosteric heat for propene adsorption in ITQ-12 than for other pure silica zeolites is ascribed to the close fit of propene in the narrow cage, evoking a cage expansion in the x direction and a strong interaction between the adsorbate and the framework.

Supporting Information Available: The crystallographic information file (CIF) of ITQ-12 with adsorbed propene as a result of Rietveld refinement on the basis of combined synchrotron X-ray and neutron diffraction. This material is available free of charge via the Internet at <http://pubs.acs.org>.

References and Notes

- (1) Keller, G. E. *Chem. Eng. Prog.* **1995**, *91*, 56.
- (2) Eldridge, R. B. *Ind. Eng. Chem. Res.* **1993**, *32*, 2208.
- (3) Rege, S. U.; Pardin, J.; Yang, R. T. *AIChE J.* **1998**, *44*, 799.
- (4) Pardin, J.; Rege, S. U.; Yang, R. T.; Cheng, L. S. *Chem. Eng. Sci.* **2000**, *55*, 4525.
- (5) Cheng I. S.; Wilson, S. T. U.S. Patent 6,293,999, 2001.
- (6) Reyes, S. C.; Krishnan, V. V.; DeMartin, G. J.; Sinfelt, J. H.; Strohmaier, K. G.; Santiesteban, J. G. U.S. Patent 6,730,142 B2, 2004.
- (7) Zhu, W.; Kapteijn, F.; Moulijn, J. A.; den Exster, M. C.; Jansen, J. C. *Langmuir* **2000**, *16*, 3322.
- (8) Olson, D. H. U.S. Patent, 6,488,741, 2002.
- (9) Olson, D. H.; Cambor, M. A.; Villaescusa, L. A.; Kuehl, G. H. *Microporous Mesoporous Mater.* **2004**, *67*, 27.
- (10) Barrett, P. A.; Boix, T.; Puche, M.; Olson, D. H.; Jordan, E.; Koller, H.; Cambor, M. A. *Chem. Commun.* **2003**, 2114.
- (11) Olson, D. H.; Yang, X.; Cambor, M. A. *J. Phys. Chem. B* **2004**, *108*, 11044.
- (12) Boix, T.; Puche, M.; Cambor, M. A.; Corma, A. U.S. Patent 6,471,939, 2002.
- (13) Grey, C. P.; Poshni, I.; Gualtieri, A. F.; Norby, P.; Hanson, J. C.; Corbin, D. R. *J. Am. Chem. Soc.* **1997**, *119*, 1981.
- (14) Ciraolo, M. F.; Hanson, J. C.; Toby, B. H.; Grey, C. P. *J. Phys. Chem. B* **2001**, *105*, 12330.
- (15) Morell, H.; Angermund, K.; Lewis, A. R.; Brouwer, D. H.; Fyfe, C. A.; Gies, H. *Chem. Mater.* **2002**, *14*, 2192.
- (16) Yang, X.; Cambor, M. A.; Lee, Y.; Liu, H.; Olson, D. H. *J. Am. Chem. Soc.* **2004**, *126*, 10403.
- (17) Larson, A.; von Dreele, R. B. *GSAS Manual*, Los Alamos Report No. LA-UR-86-748; Los Alamos National Laboratory: Los Alamos, NM, 1986.
- (18) Toby, B. H. *J. Appl. Crystallogr.* **2001**, *34*, 210.
- (19) Finger, L. W.; Cox, D. E.; Jephcoat, A. P. *J. Appl. Crystallogr.* **1994**, *27*, 892.
- (20) *Accelrys Cerius² Sorption*; Accelrys: San Diego, CA, 2003.
- (21) Cheetham, A.; Wilkinson, A. P. *Angew. Chem., Intl. Ed. Engl.* **1992**, *31*, 1557.